Thermal degradation analysis of innovative PEKK-based carbon composites for high-temperature aeronautical components

P Tadini, N Grange, Khaled Chetehouna, Nicolas Gascoin, S Senave, I Reynaud

Thermal degradation analysis of innovative PEKK-based carbon composites for high-temperature aeronautical...

Article *in* Aerospace Science and Technology · February 2017

DOI: 10.1016/j.ast.2017.02.011

CITATIONS
0

READS
56

6 authors, including:

Pietro Tadini
Université d'Orléans
20 PUBLICATIONS **80** CITATIONS
SEE PROFILE

Nathan Grange
INSA Centre Val de Loire, bourges
3 PUBLICATIONS **1** CITATION
SEE PROFILE

Khaled Chetehouna
Institut National des Sciences Appliquées Centr...
37 PUBLICATIONS **49** CITATIONS
SEE PROFILE

Nicolas Gascoin
Institut National des Sciences Appliquées Centr...
107 PUBLICATIONS **495** CITATIONS
SEE PROFILE

Thermal degradation analysis of innovative PEKK-based carbon composites for high-temperature aeronautical components

Pietro Tadini[a,1], N. Grange[b,a,2], Khaled Chetehouna[a,3], Nicolas Gascoin[a,3], S. Senave[b,4], Isabelle Reynaud[b,4]

[a] *INSA-CVL, PRISME, Univ. Orléans, 18020 Bourges, France*
[b] *DAHER, 23 Route de Tours, 41400 Saint Julien de Chedon, France*

Abstract

Nowadays, composite materials find a large application in several engineering fields, spanning from automotive to aerospace sectors. In the latter, especially in aircraft civil transportation, severe fireproof requirements must be accomplished, taking into account that the second most frequent cause of fatal accidents involving airplanes, was the post-impact fire/smoke, as reported by the European Aviation Safety Agency (EASA) in 2014. In the light of this, experimental research is of crucial importance in the understanding thermal behavior of composites for aircraft components, when exposed to high-temperature and fire conditions. In this context, a thermal degradation study is carried out for two carbon-reinforced resins: the well known thermosetting phenolic and a thermoplastic polyether-ketone-ketone (PEKK), recently developed specifically for this kind of application. The aim is to evaluate the PEKK behavior and to understand the impact of composite nature in terms of structural strength under fire. To this end, thermogravimetric analysis were performed for three different non-isothermal heating programs, between 30 and 1000 °C. Under inert atmosphere one single global reaction is observed for carbon-PEKK between 500-700

Email address: pietro.tadini@insa-cvl.fr (Pietro Tadini)
[1] Researcher
[2] PhD Candidate
[3] Professor
[4] Engineer

°C, while two for carbon-phenolic, whose pyrolysis begins around 200 °C. This better PEKK strengthening is attributed to the ether and ketone bonds between the three aromatic groups of the monomer. As expected, under oxidative atmosphere, the kinetic process becomes more complex, making more difficult the detecting of single-step reactions, especially for carbon-phenolic. Nevertheless, the oxidative process of carbon-PEKK seems to be driven by three consecutive global reactions. The activation energy is estimated by means of both integral (Starink) and differential (Friedman) isoconversional methods, as a function of the extent of conversion, corresponding to the identified reaction intervals. For carbon-PEKK in inert conditions, with Starink a mean value of 207.71 ± 6.57 kJ/mol was estimated, while 213.88 ± 20.04 kJ/mol with Friedman. This expected slight difference depends on the nature of the considered mathematical approaches. The difficulty in activation energy estimation for polymeric materials prefers the use of at least two different methods, allowing for the identification of an activation energy range, for a resin of which no data are available in the literature. For the decomposition model evaluation, the so called compensation effect method was implemented, as well as the single-step-based approach proposed by Friedman. The evaluation of a possible decomposition expression has been achieved only for carbon-PEKK under inert conditions, since the considered methods are valid and applicable only for well defined single-step reactions. In fact, the three reactions of the oxidative case cannot be considered as single-step processes. Moreover, the higher difference in the estimated activation energy between Starink and Friedman suggests to check the achieved results by implementing further isoconversional methods, to understand the most reliable for polymer-based carbon composites degradation analysis under oxidative atmosphere. However, the observed higher thermal performance of PEKK resin, attributed to its chemical structure, increases the interest toward its use as matrix for aerospace composite materials, that can be subjected to hazardous environments.

Keywords: aircraft composites, fire safety, thermal degradation, kinetic

analysis, advanced materials

1. Introduction

Nowadays, composite materials are widely employed in several engineering fields, spanning from automotive to aerospace sectors. In the latter, the need of mass reduction, high resistance to corrosion and, in the meantime, increase of structural performance make the use of composites extremely important, endorsing the research and the development of new materials [1]. For instance, approximately the 50% in mass of the Boeing 787 Dreamliner is made by carbon-reinforced composites; in this sense, another example is the Airbus A350-XWB with 52% in mass [2], as well as the Bombardier CSeries with a percentage of 47% [3]. Besides the high structural performance requirements, that must be satisfied in civil aerospace field, a high-level standard is also required for what concern the aviation safety. In 2014, according to the Annual Safety Review, edited by the European Aviation Safety Agency (EASA), the second most frequent cause of fatal accidents, involving airplanes, was the post-impact fire/smoke [4]. In the light of this, experimental research is of crucial importance to understand the thermal behavior of composites exposed to high-temperature and hazardous fire aggression, thus improving the ability to predict their thermo-structural behavior [5, 6], when employed as aeronautical system components, or, at industrial level, as fire barriers and other power-plant systems [7, 8]. Actual standards, such as the ISO 2685 [9] and the AC20-135, of US Federal Aviation Administration (FAA) [10], define very severe fireproof requirements, to simulate a realistic scenario of an in-service or post-impact fire event, for aircraft parts dedicated to firewall applications or located in potential fire zones. In fact, the composite components are subjected to temperatures up to 800 °C for long time, causing initially the decomposition of the material and then its combustion. Nevertheless, after a fire test, composite specimens still present a residual structural strength, which, on the contrary, is totally lost by classical aluminum alloys [11]. Such property represents strong advan-

tage in term of structural performance and fire safety, avoiding the need of high temperature resistance, but significantly heavier, metals [12]. However, due to their heterogeneity, the degradation process of composite materials results very complex and characterized by the occurring of multi-step chemical reactions, char formation and physical phenomena, like delamination, which, modifying the geometrical structure, has a direct impact on the heat transfer in the solid material. The chemical decomposition of resin is the first step of the degradation; if one thinks about a composites flat panel, the surface side exposed to high-temperature conditions will release pyrolysis gases and produce char, going to change the thermophysical properties, such as porosity and heat exchange, in the inner layer of the material [13]. The resin decomposition reduces also the grip between fibers, so allowing carbon sheets delamination, especially if the component is also subjected to mechanical stress. In the case of carbon-reinforced composites, the chemical behavior can strongly differ between different polymer resins. Indeed, the latter must be accurately selected, taking into account structural, aerodynamics and thermal requirements. Depending on the specific application, aircraft parts can be even marked out by complex design, thus increasing the need of high quality preliminary analysis. In this context, computational fluid dynamics (CFD) represents a useful approach for the comprehension of composite components degradation behavior, subjected to simulated fire conditions [14]. However, the computational study, besides flame and flow field characteristics, requires the knowledge of material properties, as well as its decomposition model. To this end, the considered materials must be characterized experimentally, typically with differential scanning calorimetry (DSC), flash pyrolysis and thermogravimetric analysis (TG) [15, 16, 17]. In particular, the latter, consisting in the mass loss measurement during a specific heating program inside a furnace, is able to highlight the main reactions that occur during the degradation process, providing an overall description of the kinetic mechanism [18]. With the achieved experimental data, the activation energy of a specific reaction can be estimated by means of model-free isoconversional methods, obtaining then a complete kinetic triplet, made by activation

energy, preexponential factor and reaction model [19]. In recent years, a large number of studies have been released to investigate the relationship between fire events and composites degradation kinetics [20, 21, 22, 23]. However, a lot is still to do due to the non-determinist process of fabrication of composite materials. Indeed, as suggested by the European Material and Modeling Council (an initiative of the European Commission grouping all stakeholders of the related communities), even metal materials present inclusion and local failure that make their behavior difficult to predict [24]. Composite materials are even worst in terms of variability from one to another. Thus, this work aims to contribute to the ongoing global research, by dealing with the thermogravimetric analysis of two polymer resins, reinforced with carbon fibers: a thermosetting phenolic [25], widely used as thermal protection [26, 27, 28], here considered for comparison purpose with the less known thermoplastic polyether-ketone-ketone (PEKK), belonging to the family of polyaryletherketone (PAEK) known for its high-temperature stability [29]. The comprehension of PEKK behavior, as well as the impact of composite nature, in terms of structural strength and thermal response under fire [30] might represent a key step for scientific and engineering community. The two materials have been tested in both oxidative and inert atmosphere, under three different non-isothermal heating programs. Such kind of experimental study can provide a preliminary comprehension of the degradation mechanism of carbon-PEKK composite, useful in the perspective of degradation model implementation within a CFD code for fire conditions simulation. In Section 2, the materials and the experimental apparatus are described, whereas in Section 3 a synthetic overview on most commonly used isoconversional methods is proposed. Finally, in Section 4, the TG measurements and the results in kinetic parameter estimation are presented, for both inert and oxidative cases, with the addition of scanning electron microscope (SEM) visualizations on the two materials before and after the inert TG experiments.

2. Materials and Methods

2.1. Materials

Two carbon-reinforced ($7\mu m$ fiber dia) polymer resins are considered: a thermosetting phenolic and a thermoplastic PEKK. The former is a well known resin, typically employed as carbon-composites thermal protection, such as in rocket nozzles [26], as thermal shields for spacecraft atmospheric reentry [28] but even for components in automotive [31] and as fire barriers in naval applications [32]. The phenolic resin is produced by a polymerization reaction between phenol C_6H_6OH (or carbolic acid) and formaldehyde, see Figure 1.

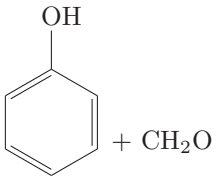

Figure 1: Phenol and formaldehyde link, result of phenolic polymerization reaction.

The former is an aromatic compound made by phenyl and a hydroxyl group (-OH), while the second is the well known organic compound CH_2O. A detailed description of the material and its polymerization process is available in [33, 34]. Phenolic belongs to the class of slow-ignite resins; when exposed to fire, its decomposition yield a high amount of char (up to 50% of the initial mass) and low amount of flammable volatiles. In addition, once ignited it is easy to be extinguished [31, 33]. Due to these properties, phenolic-based composites represent an excellent solution for thermal protection in high-temperature environments.

Polyether-ketone-ketone (PEKK) is a semi-crystalline thermoplastic material belonging to the family of polyaryletherketone (PAEK), known for their high mechanical performance and high temperature stability [35, 29, 36]. PEKK-based composites find their main use in aerospace applications [37, 36], especially for exterior structures and cabin interiors, due to their low flammability and smoke emission when subjected to fire [38]. The PEKK monomer is characterized by three aromatic groups bonded together by ether ($R--O--R'$) and

ketone ($RC(=O)R'$) links, see Figure 2. More details on the PEKK structure and its synthesis are provided in [39, 40].

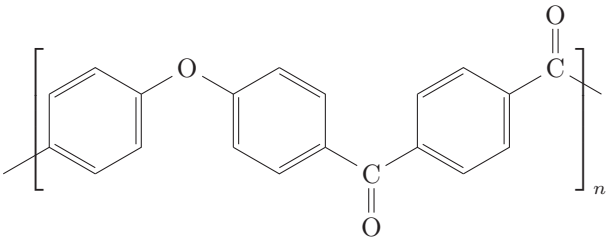

Figure 2: Polyether-ketone-ketone monomer schematic.

Similarly to phenolic, also PEKK yields a large amount of char ($\sim$ 60 % of initial mass) due to the high concentration of aromatic groups [33, 41], but, on the contrary, it shows a significant higher thermal resistance (glass transition and melting temperatures are $T_g = 156$ °C and $T_m = 338$ °C respectively [39]). Because of this, PEKK-based composites are mainly use for components whose priority is mechanical performance under high-temperature or fire conditions.

2.2. Measuring Apparatus

Thermogravimetric measures were performed with a SETARAM Setsys-16/18 TG, both in oxidative (air) and inert (argon) conditions at atmospheric pressure. This device consists of a vertical-type TG where the Al_2O_3 crucible is hung to the electronically controlled balance. All the experiments were carried out with an argon and air flow rate of, respectively, 16.6 ml/min and 15.0 ml/min. In order to achieve a good compromise between experiments schedule and accuracy of results, three non-isothermal heating rates were considered: 5, 15 and 25 $°C/min$. Once loaded the sample, a high argon flow rate cycle was used for the purge of the whole setup, before the beginning of the heating phase, at ambient temperature. The final temperature was fixed at 1000 °C, followed by an isothermal phase of 10 minutes before the cooling phase.

For both phenolic and PEKK composites, the samples were prepared in form of particulate, directly crashed from the virgin piece (1.5 mm thick plate). This allowed an easy crucible loading and a uniform sample distribution on the

Sample Masses [mg]				
	Carbon-phenolic		**Carbon-PEKK**	
β [$^{\circ}C/min$]	Argon	Air	Argon	Air
5	7.86	8.17	8.56	7.98
15	8.07	8.07	7.75	7.93
25	7.87	8.03	8.62	7.93

Table 1: Initial sample masses and heating rates used for thermogravimetric analysis.

crucible bottom. Masses between 7-9 mg were considered, in order to limit the temperature gradients in the sample and minimize temperature deviation with respect to the furnace. In addition, such mass range should assure a good distribution of the sample elements. In fact, composite materials are strongly heterogeneous, thus too small sample masses might present a poor amount of some elements [18]. In Table 1 the initial masses of the samples for the TG experiments are reported, with regard to the heating rates.

3. Thermal Data Analysis

3.1. Reaction Rate in Solids

The decomposition rate of solids is described, in the general form [19], as a function of temperature T, pressure P and extent of conversion α

$$\frac{d\alpha}{dt} = K(T)f(\alpha)h(P) \tag{1}$$

where $K(T)$ is the reaction rate, $f(\alpha)$ is the reaction model and $h(P)$ accounts for pressure dependence. The latter is generally ignored in the frame of thermogravimetric analysis, where $h(P)$ is assumed constant, with no pressure influence of the kinetic process, if the gaseous products are efficiently removed during the experiments [19]. On the other hand, the temperature dependence of the reaction rate $K(T)$ is typically expressed by means of the Arrhenius equation [42, 19]

$$\frac{d\alpha}{dt} = A\ exp\left(\frac{-E}{RT}\right) f(\alpha) \tag{2}$$

where A is the preexponential, or frequency, factor, E is the activation energy, T is the absolute temperature and R is the gas constant. In the case of thermogravimetric analysis, α is defined as

$$\alpha = \frac{m(t) - m_0}{m_\infty - m_0} \tag{3}$$

where m is the mass at the time t, m_0 is the initial mass and m_∞ is the mass at the end of the thermal degradation process [43, 18] of the specific sample and heating rate. This mass value is identified by plotting the dm/dT data and observing the temperature at which the derivative drops back to zero. In order to account for non-isothermal heating programs, the reaction rate can be expressed as a function of temperature

$$\frac{d\alpha}{dT} = \frac{d\alpha}{dt}\frac{dt}{dT} \tag{4}$$

where dT/dt is the heating rate β, and substituted in Eq. 2, obtaining the non-isothermal differential rate law

$$\frac{d\alpha}{dT} = \frac{A}{\beta} exp\left(\frac{-E}{RT}\right) f(\alpha) \tag{5}$$

By separating variables and integrating, one can obtain the integral form

$$g(\alpha) \equiv \int_0^\alpha \frac{d\alpha}{f(\alpha)} = \frac{A}{\beta}\int_0^T exp\left(\frac{-E}{RT}\right) dT \tag{6}$$

in which the temperature integral has not an analytical solution and it should be solved by means of approximation functions or numerical integration [44].

3.2. Isoconversional Methods

An isoconversional method assumes that the reaction rate at a constant extent of conversion α is only function of temperature [19]. This assumption allows for the estimation of the activation energy E without the need to consider a specific reaction model $f(\alpha)$. In practice, the temperature dependence of

the isoconversional rate is obtained by performing 3-5 runs at different heating rates [19, 44]; each extent of conversion α_i corresponds to a temperature range ΔT_i delimited within the heating rates considered. Thus, by means of different computational methods, one can evaluate the activation energy, E_α, as a function of the extent of conversion, detecting the occurring of single- or multi-step reactions. In fact, a negligible dependence of E_α on α is related to the presence of a dominant single-step reaction. On the contrary, the degradation process is characterized by a more complex kinetics, with multi-step reactions [19, 44]. This is the case of polymer-based composite materials, whose E curve shows typically different shoulders highlighting the complexity of the decomposition mechanism. In particular, the activation energy of polymers was observed to increase as the conversion proceeds, due to the increase of the residual material refractory level [19]. It is important to remember that, despite the identification of a specific reaction model is not required for E_α estimation, the conversion rate is assumed obeying to a $f(\alpha)$ model. In any case, the latter is required for the evaluation of the preexponential factor, in order to describe the single-step reaction by a complete kinetic triplet (i.e. E, A, $f(\alpha)$). Of course, one must consider different kinetic triplets to describe the reactions included in a multi-step decomposition process.

Isoconversional methods are divided in two categories, differential and integral, depending on the type of experimental data. Among the first category, the most used is Friedman method [45], originally proposed for the study of polymeric materials and largely accepted by the scientific community, based on the following expression, valid for non-isothermal heating programs

$$ln\left[\beta_i\left(\frac{d\alpha}{dT}\right)_{\alpha,i}\right] = ln\left[f(\alpha)A_\alpha\right] - \frac{E_\alpha}{RT_\alpha}\ . \tag{7}$$

By means of Eq. 7, the activation energy E_α is calculated as the slope of the linear regression of the differential experimental data plotted as $ln(\beta_j(d\alpha/dT)_i)$ on $1/T_i$, for all heating rates j and each α_i [45, 19, 44].

On the other hand, integral methods apply the isoconversional principle to

Eq. 6, whose integral has not an analytical solution in relation to an arbitrary temperature program [46, 47, 19, 44]. Different approximation functions were proposed to replace the temperature integral, thus originating different isoconversional methods. As demonstrated by Starink [47], such methods can be represented by the following general linear expression

$$ln\left(\frac{\beta_j}{T^B_{\alpha,i}}\right) = Const - C\left(\frac{E_\alpha}{RT_\alpha}\right) \tag{8}$$

where B and C are parameters that depend on the integral approximation considered. In Table 2, one can see the corresponding parameters for the most used methods, Ozawa-Flynn-Wall [46], Kissinger-Akahira-Sunose (KAS) and Starink [47]. In the latter, the parameters are optimized for the best accuracy on activation energy estimation. In general, the Ozawa-Flynn-Wall offers the lowest accuracy, since it is based on a very crude approximation.

Method	**Approx**	**B**	**C**
Ozawa-Flynn-Wall	Doyle	0	1.052
Kissinger-Akahira-Sunose (KAS)	Murray-White	2	1
Starink	Optimized Parameters	1.92	1.0008

Table 2: Parameters for the general integral isoconversional equation developed by Starink [46, 47, 19, 44]

Better results are achieved with KAS method and, in particular, with Starink parameters [19, 44]. Similarly to Friedman method, each $E_{\alpha,i}$ corresponds to the slope of the linear regression applied on the integral experimental data plotted as $ln\left(\beta_j/T^B_{\alpha,i}\right)$ on $1/T_i$, for all beta j, as represented in Figure 3.

The need of an approximation function makes this kind of integral methods potentially less accurate than differential approaches. Nevertheless, small noise in TG mass measure is emphasized in derivative data dm/dt, requiring the need of smoothing, thus introducing a source of inaccuracy. Therefore, generally, integral methods are preferred for activation energy estimation and more recent approaches exploits the numerical integration of the temperature integral, in

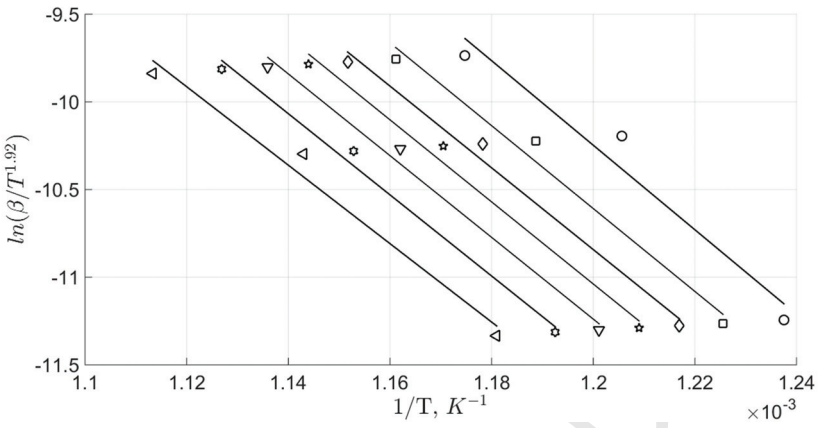

Figure 3: Example of Arrhenius-type plot for activation energy estimation with Starink method [47]. The slope of linear regression on the experimental data couples (dots) of three different beta corresponds to $E_{\alpha,i}$.

order to go beyond the inaccuracy introduced by the use of an approximation function [19, 44]. For the purpose of this work, the classic Friedman and Starink methods were implemented and compared, in order to identify an estimation range for the activation energy.

3.3. Kinetic Triplet and Reaction Models

Once determined the activation energy, one must complete the reaction description by the evaluation of the preexponential factor A and reaction model $f(\alpha)$. A correct estimation of these parameters is possible when the degradation process can be described by a single-step dominant reaction. This happens when E_α does not significantly vary with the extent of conversion; typically accepted when the difference ΔE_α, between the maximum and minimum values, is within the 10% of the mean activation energy [44]. If this condition is accomplished, the kinetic triplet can be evaluated with the approach of invariant kinetic parameters or also called *compensation effect* method [19, 44]. By taking the natural logarithm of Eq. 5 and fitting the curve with the experimental data of each β_j, it is possible to obtain a couple (lnA_i,E_i) for each reaction model $f(\alpha)_i$ considered. The different pairs calculated show a strong linear correlation

$$lnA_i = a_j E_i + b_j \tag{9}$$

known as compensation effect, where a_j and b_j are parameters that depend on the heating rate. Then, if the correct model is not included, one can use the Eq. 9, for any β_j, to estimate the preexponential factor corresponding to the mean activation energy $\bar{E}_\alpha$ determined with the isoconversional method. In fact, the heating rate does not affect the value of A_α, despite negligible variations can be observed using different β_j [44]. Finally, the calculated values are used to reconstruct the reaction model, both integral and differential

$$g(\alpha) = \frac{A_\alpha}{\beta} \int_0^{T_\alpha} exp\left(\frac{-\bar{E}_\alpha}{RT}\right) dT \tag{10}$$

$$f(\alpha) = \beta \left(\frac{d\alpha}{dT}\right)_\alpha \left[A_\alpha exp\left(\frac{-\bar{E}_\alpha}{RT_\alpha}\right)\right]^{-1} \tag{11}$$

By comparing the plot of Eqs. 10-11 against different theoretical models, the kinetic triplet can be obtained or, at least, useful indications on the type of reaction. In Table 3, the most common used reaction models for solid-state kinetic are reported, organized in four categories: nucleation, geometrical, diffusion and reaction-order. Another largely used approach is that proposed by Friedman, based on the generic n-order reaction expression $f(\alpha) = (1-\alpha)^n$, typically assumed for polymer materials. A detailed description of preexponential factor and n-order estimation is provided in [45].

The described approaches lose their validity when the isoconversional activation energy shows a significant variation with α, highlighting the occurring of a multi-step decomposition kinetic. In such a case, it is necessary to identify and analyze singularly the different reactions, thus estimating a corresponding number of kinetic triplets. Nevertheless, this is not always easy, especially in the study of polymer-based materials, due to the high complexity of their kinetic mechanism, which increases the difficulty of single-step reactions identification. An alternative approach for multi-step kinetic detection is offered by model-fitting methods, based on non-linear minimization of the difference between the

Reaction Model	Code	Type	$\mathbf{f}(\alpha)$	$\mathbf{g}(\alpha)$
Power law	P2	nucleation	$2\alpha^{1/2}$	$\alpha^{1/2}$
Power law	P3	nucleation	$3\alpha^{2/3}$	$\alpha^{1/3}$
Avrami-Eforeev	A2	nucleation	$2(1-\alpha)[-ln(1-\alpha)]^{1/2}$	$[-ln(1-\alpha)]^{1/2}$
Avrami-Eforeev	A3	nucleation	$3(1-\alpha)[-ln(1-\alpha)]^{2/3}$	$[-ln(1-\alpha)]^{2/3}$
Contracting Cylinder	R2	geometrical	$2(1-\alpha)^{1/2}$	$1-(1-\alpha)^{1/2}$
Contracting Sphere	R3	geometrical	$3(1-\alpha)^{2/3}$	$1-(1-\alpha)^{2/3}$
1D diffusion	D1	diffusion	$1/2\alpha$	α^2
2D diffusion	D2	diffusion	$-[1/ln(1-\alpha)]$	$[(1-\alpha)ln(1-\alpha)]+\alpha$
3D diffusion	D3	diffusion	$[3(1-\alpha)^{2/3}]/[2(1-(1-\alpha)^{1/3})]$	$1-(2/3)\alpha-(1-\alpha)^{2/3}$
0th order	F0/R1	reaction-order	1	α
Manpel	F1	reaction-order	$(1-\alpha)$	$-ln(1-\alpha)$
2nd order	F2	reaction-order	$(1-\alpha)^2$	$[1/(1-\alpha)]-1$

Table 3: Some kinetic models generally considered in the study of solid-state decomposition [19, 42]

experimental measured reaction rate and the calculated one [19]. The latter methods category is not considered in this work, focusing the attention on the isoconversial methods proposed by Friedman and Starink.

4. Results and Discussion

In this section, the experimental measures carried out at different heating-rates are presented and discussed by comparing the two materials in both inert and oxidative atmospheres. In addition, the activation energy is estimated and, when possible, the kinetic triplet for dominant reactions is evaluated.

4.1. Inert Atmosphere

In Figure 4, one can see the mass loss curves of carbon-phenolic and carbon-PEKK, subjected to three different non-isothermal heating rates. Both resins are characterized by a mass release of about 20%, whereas an important different exists regard the beginning of degradation and its development rate. In fact, the degradation of carbon-phenolic begins around 200 °C, proceeding slowly up to about 900 °C. Moreover, it seems evident the presence of at least two main reactions, associated with the change of slope curve: the first between 200 and 400 °C and the second between 400 and 900 °C. On the other hand, the carbon-PEKK does not present any mass variation up to about 515 °C; then a faster

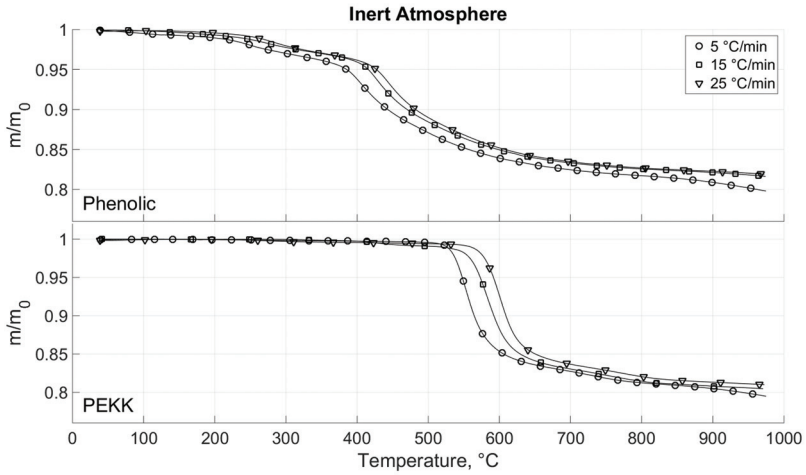

Figure 4: Mass loss curves obtained for β equal to 5, 15 and 25 °C in inert atmosphere. Comparison between carbon-phenolic and carbon-PEKK.

degradation process occurs highlighting one global reaction, which comes to end at about 900 °C. In Figure 5, the derivative TG curves (DTG) are reported, for both the tested materials and all non-isothermal heating rates, under inert atmosphere.

Derivative data emphasize the presence of different reactions, each one associated with a peak. Nevertheless, depending on the material complexity, a detailed reaction identification might be difficult, allowing to observe only the dominant and slowest reactions that drive the degradation process. In addition, since the characteristic time of a decomposition reaction, dependent on sample and temperature, is not affected by the heating rate, in Figure 5, one can observe the typical peaks shifting toward higher temperature with the increase of β [18, 43], for both the materials. In Table 4, the peaks corresponding temperatures are reported. The DTG curves, presented in Figure 5, confirm the reaction sequence observed in Figure 4 for the tested materials. With regard to carbon-phenolic, two peaks are visible, in agreement with the literature: the first, occurred between 200-300 °C and characterized by a mass loss of about 5%, is associated with resin dehydration [33] and release of non-reacted com-

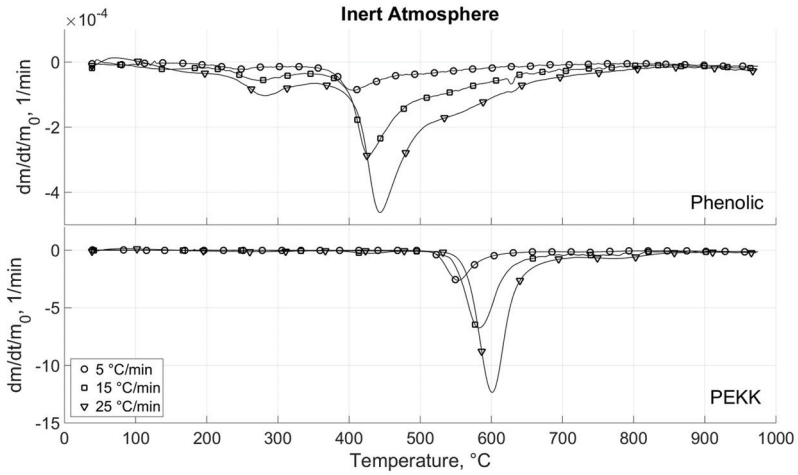

Figure 5: DTG curves obtained for β equal to 5, 15 and 25 °C in inert atmosphere. Comparison between carbon-phenolic and carbon-PEKK.

ponents (i.e. phenol and formaldehyde trapped between polymer chains during the curing process) [34].

β	**Carbon-phenolic**		**Carbon-PEKK**
$[°C/min]$	reac. 1	reac. 2	reac. 1
5	250	397	553
15	272	425	581
25	280	442	600

Table 4: Peaks corresponding temperatures ($°C$) from DTG curves, under inert conditions, for carbon-phenolic and carbon-PEKK.

The second, occurred between 400-650 °C and characterized by the greatest mass reduction, is associated with random chains scission, with no any resin de-polymerization, and release of various compounds, such as phenol, cresols, water, carbon monoxide, carbon dioxide and methane. It is important to note that the high content of oxygen in phenolic resins can promote thermo-oxidative processes even if the decomposition occurs under inert atmosphere [34]. By focusing the attention on Figure 5, after the second peak, one can see a significant

slope decrease following an inflection point clearly visible around 510 °C for $\beta = 25\ °C/min$. The same trend is shown by the other two heating rates, with a shifted temperature inflection point. This change of slope might be theoretically due to the presence of a further reaction, largely overlapped with the previous ones. Although, in first approximation, one might associate this behavior with thermo-oxidative phenomena due to oxygen release during phenolic decomposition, further tests at different heating rates should be preferable for a better comprehension. On the other hand, carbon-PEKK DTG curve confirms the evidence of one dominant single-step reaction, characterized by higher intensity peaks due to the higher rate of conversion, see Figure 5. Similar behavior is reported in the literature for composites with Poly-ether-ether-ketone (PEEK) resin, which belongs to the PEAK family [38, 41]. The identified reaction lies between about 510-710 °C and it might be associated with the random scission of ether bonds, as described in [33]. In particular, the decomposition process is expected to begin with the rupture of weakest bonds between the aromatic groups, whereas the major volatiles release should consists of phenol [41]. The onset of this decomposition occurs after the transition phase of PEKK resin, typically observed by DSC measurements around 340 °C [39].

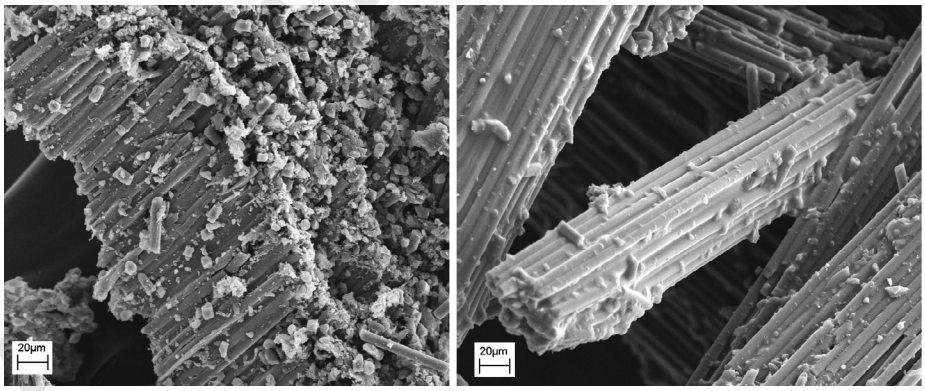

Figure 6: SEM visualization of carbon-PEKK crashed sample before (left) and after (right) the TG experiment under inert conditions and heating rate of 15 $°C/min$.

In Figure 6, one can see the SEM images of carbon-PEKK sample before

(Figure 6 left) and after (Figure 6 right) the TG experiment. In the observed section of the crashed virgin material, it is clearly visible the orientation of the fibers, that are fully merged with PEKK matrix. However, some fibers appear more or totally exposed, allowing their diameter measure. On the contrary, after the TG test, for the observed sample element, the decomposition of a part of the resin, associated with the identified single-step global reaction, permits an easier visualization of the fibers, arranged in a sort of bundles. The latter, accordingly to the thermoplastic nature of PEKK, are banded together by the not decomposed re-crystallized resin, which fulfills the interstices between fibers, providing this smoothed glued aspect. SEM visualizations of the carbon-phenolic crushed sample is presented in Figure 7. In this case, the difference between the material before (Figure 7 left) and after (Figure 7 right) the TG test is less evident.

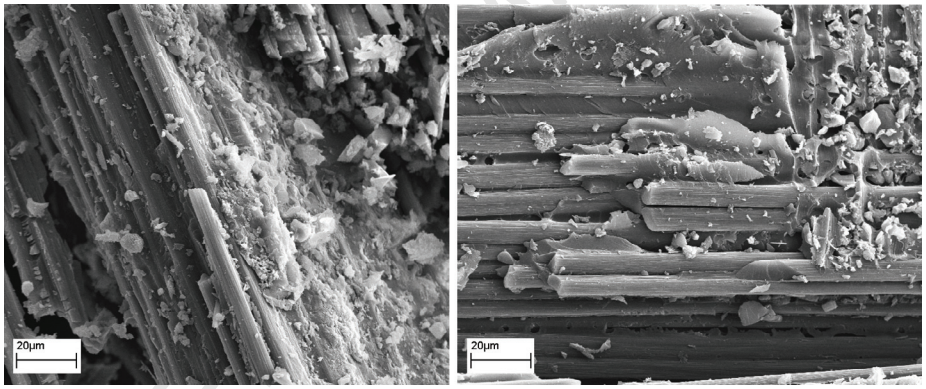

Figure 7: SEM visualization of carbon-phenolic material before (left) and after (right) the TG experiment under inert conditions and heating rate of 15 $°C/min$.

What one can observe is a more uniform distribution of the thermosetting resin around the fibers, whereas, after the degradation, some regions remain more exposed allowing to clearly see the carbon fibers and the empty interstices between them. Because of the thermosetting nature of phenolic, any matrix re-crystallization occurs.

4.2. Oxidative Atmosphere

The TG experimental data are reported in Figure 8, where carbon-phenolic and carbon-PEKK are compared under oxidative atmosphere. In such condition, all samples have been almost completely consumed. As for inert atmosphere, the degradation of carbon-phenolic begins after 200 °C and concludes between 740-800 °C, depending on the heating rate of the test.

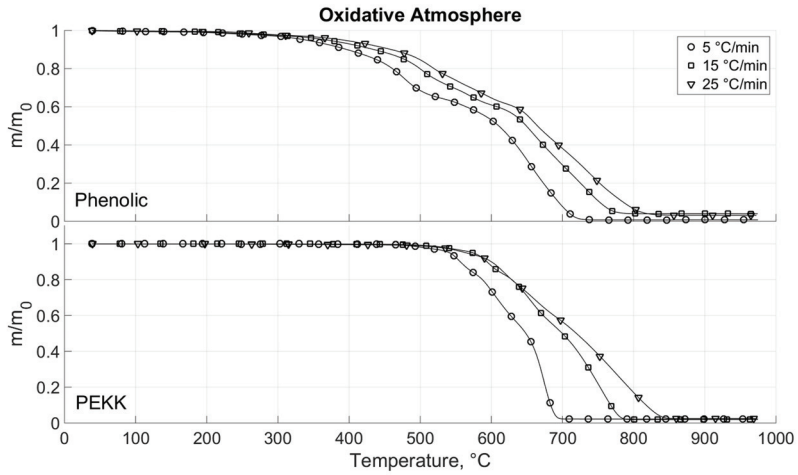

Figure 8: Mass loss curves obtained for β equal to 5, 15 and 25 °C in oxidative atmosphere. Comparison between carbon-phenolic and carbon-PEKK.

Four inflection points are visible in the TG curve underlining the occurring of a complex reaction pattern. The same complexity is observed for carbon-PEKK, whose degradation starts at about 500 °C to conclude between 700-850 °C. In Figure 9, one can see the DTG data under oxidative atmosphere. Focusing the attention on carbon-phenolic, it is possible to see the resin dehydration between 200-300 °C, followed by a large peak between 475-515 °C, depending on the heating rate. The latter, might correspond to the resin decomposition reaction, despite shifted toward higher temperature with respect to the inert atmosphere case. After this peak, the derivative data are characterized by several other peaks of different intensity, underlining the high complexity of the kinetic mechanism in oxidative case, characterized by multi-step reactions, and

hampering the identification of few global reactions. The presence of a complex peak pattern seems more evident for heating rates of 15-25 °C/min, while the curve at 5 °C/min reveals only two large peaks after the dehydration one (see Figure 9).

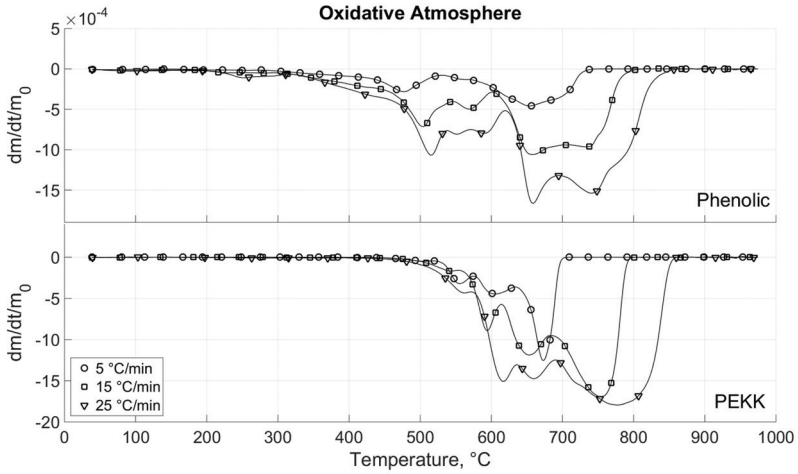

Figure 9: DTG curves obtained for β equal to 5, 15 and 25 °C in oxidative atmosphere. Comparison between carbon-phenolic and carbon-PEKK.

On the other hand, all the carbon-PEKK experimental curves present three main peaks, whose temperatures are reported in Table 5, leading to suppose a process described by three global reactions. The first might be associated with resin decomposition, since it occurs in correspondence of the same temperatures observed in inert conditions, between 550-615 °C, depending on the heating rate. The second appears between 575-689 °C while the third follows between 633-862 °C. These peaks might refer to the combustion of carbon fibers, whose onset is expected between 600-700 °C, which develops simultaneously with the decomposition and combustion of the resin, as well as that of char [41, 48]. To be noted that, before the first reaction-peak, especially evident for β 15-25 °C/min, one can see a less intense peak, almost overlapped with the former. It might be eventually due to the oxidation of the pyrolysis products released by the early scission of the weakest bonds [41] between the aromatics groups of

which PEKK resin is composed. However, also for carbon-PEKK, the observed peaks appear partially overlapped, showing a complex kinetic mechanism, so the occurring of multi-step reactions.

β	**Carbon-PEKK**		
$[°C/min]$	reac. 1	reac. 2	reac. 3
5	503	555	607
15	537	593	654
25	559	616	776

Table 5: Peaks corresponding temperatures ($°C$) from DTG curves, under oxidative conditions, for carbon-PEKK.

4.3. Kinetic Analysis

Two isoconversional methods have been implemented for the kinetic analysis of the tested materials: the differential method of Friedman and the integral method of Starink. In Figures 10 - 11, one can see the estimated activation energy E_α as a function of the extent of conversion α of carbon-phenolic and carbon-PEKK respectively. As recommended in the literature [19], the activation energy is evaluated in a wide range of α, between 0.1 and 0.9. A certain difference is observed between Friedman and Starink results, the former, as expected, shows a high sensitivity to differential data while Starink provides significantly lower oscillations on E_α values. Carbon-phenolic presents a growing activation energy trend, varying from 160 kJ/mol to about 280 kJ/mol. Such behavior has been already observed for polymer materials and associated with the refractory level increase of the residual material [19]. Large oscillations are observed in correspondence of the α interval extremes especially for Friedman. The dehydration reaction, expected between 200-300 °C, corresponds approximately, in Figure 10, to the activation energy between 0.1 and 0.2, whereas the phenolic resin decomposition reaction falls between about 0.2 and 0.65. The latter α extreme is assumed in correspondence of the inflection point in the DTG curve of Figure 5, followed by a slope change down to the return of the

derivative to zero. The corresponding E_α, from 0.7 to 0.9, are supposed, in first approximation, related to thermo-oxidative phenomena due to oxygen released during phenolic pyrolysis.

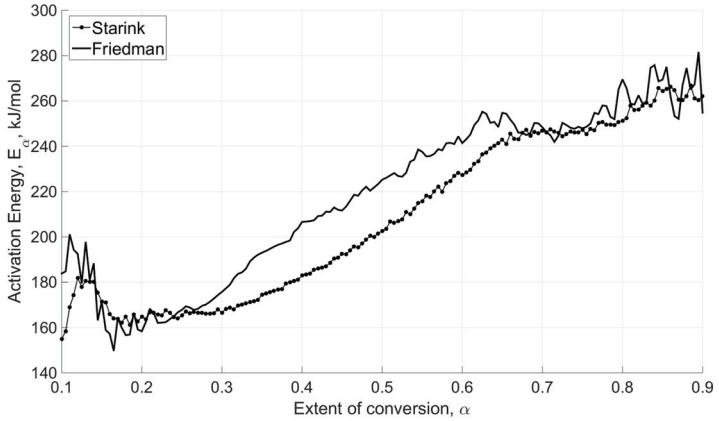

Figure 10: Activation energy vs. extent of conversion estimated by isoconversional methods for carbon-phenolic in inert atmosphere.

The calculated activation energy presents an acceptable agreement with that estimated by Friedman for glass-phenolic, 242 kJ/mol as average value of eleven points on the total degradation process [45]. However, the corresponding average E_α calculated for carbon-phenolic results 14% (207 kJ/mol) and 10% (217 kJ/mol) smaller, respectively evaluated with Starink and Friedman method.

Differently from carbon-phenolic, carbon-PEKK presents a more constant activation energy for α between 0.1 and 0.8, characterized by a slight growing of E_α, more emphasized by Friedman method starting from approximately 180 kJ/mol to maximum of about 250 kJ/mol. Such behavior was typically observed for polymer materials, whose degradation begins with the breaking of weakest links to proceed with regular bonds that require higher energy [44, 41]. In this constant range, the difference between the minimum and the a maximum values results approximately the 10% of the corresponding average $\bar{E}_\alpha$ calculated with Starink, allowing to assume that the degradation process is driven by a single-

step dominant reaction, as suggested in [19, 44]. On the other hand, Friedman presents a percentage higher than 10%, but, taking to account the typical trend of polymers activation energy, it is reasonably possible to assume the occurring of one global single step reaction. In the case of carbon-phenolic, such condition is never satisfied in the α intervals corresponding to the observed DTG peaks (Figure 5), probably revealing the occurring of multi-step reactions, as expected for such kind of heterogeneous materials.

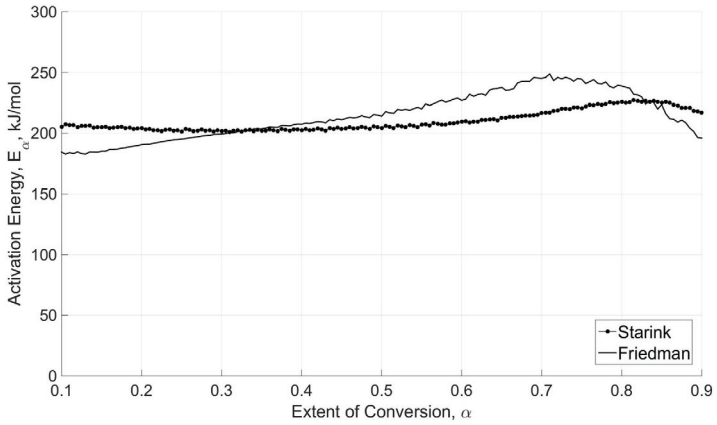

Figure 11: Activation energy vs. extent of conversion estimated by isoconversional methods for carbon-PEKK in inert atmosphere.

Focusing the attention on isoconversional methods, Friedman presents a good match with Starink results for carbon-phenolic, see Figure 10, despite a slight overestimation for α between 0.27-0.67. On the contrary, for carbon-PEKK, Friedman overestimates E_α with respect to Starink, despite an initial underestimation up to $\alpha = 0.3$, see Figure 11. However, the estimated activation energy range for carbon-PEKK results of the same order of that presented in literature for PEEK, belonging to the same resin family [49], achieving 207.71 $\pm$ 6.57 kJ/mol with Starink and 213.88 $\pm$ 20.04 kJ/mol with Friedman, for the single global reaction observed in inert conditions.

In Figure 12, the isoconversional activation energy is presented for carbon-phenolic in oxidative atmosphere. The complex decomposition kinetics revealed

by DTG data, in Figure 9, produces a significant dependency of E_α on α, for both Friedman and Starink methods, making difficult to accurately identify any single-step reactions. Moreover, Friedman shows stronger oscillations of the results with respect to Starink, which applies an approximation function for the temperature integral of Eq. 6. In Figure 13, the carbon-PEKK activation energy calculated with Starink is reported and characterized by a quasi-linear decreasing trend, whereas Friedman presents, again, more oscillating values, following the trend of differential experimental data. The significant variation of E_α under oxidative conditions, for both the tested materials, suggests the occurring of a complex degradation process characterized by multi-step reactions, despite carbon-PEKK DTG data lead to suppose a degradation process driven by three global reactions.

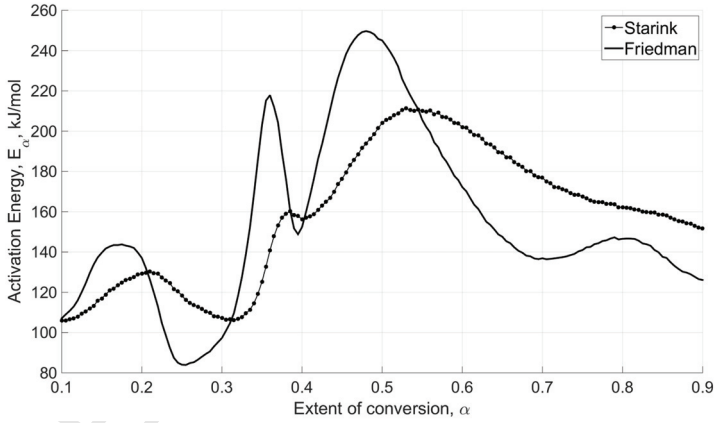

Figure 12: Activation energy vs. extent of conversion estimated by isoconversional methods for carbon-phenolic in oxidative atmosphere.

These correspond, respectively, to the following extent of conversion intervals: first reaction up to 0.19, the second between 0.19-0.43, while the third from about 0.43 to unity, as one can see in Figure 13. The extremes of these intervals are arbitrarily identified in correspondence of the DTG inflection points between the observed peaks, in Figure 9. However, except for the onset and the end of the degradation process, these α values might not coincide with the

exact begin/end of the single reactions, due to the partial overlapping of the peaks, especially for the second one, associated with the onset of carbon-fibers combustion. In Table 6, one can see the mean activation energy estimated in corresponding of the defined α intervals for the three reactions of carbon-PEKK under oxidative atmosphere. In this case, the results calculated with Friedman present a very high standard deviation, due to the strong variation of the isoconversional activation energy within the three corresponding reaction intervals.

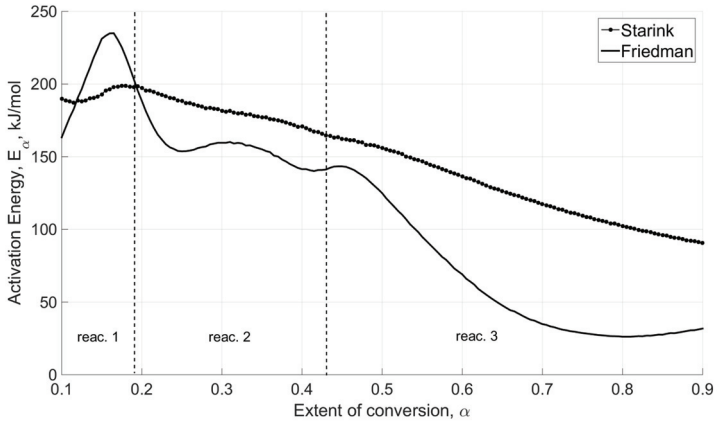

Figure 13: Activation energy vs. extent of conversion estimated by isoconversional methods for carbon-PEKK in oxidative atmosphere. The dashed vertical lines delimit the defined reaction intervals.

Less dispersed values are achieved with Starink: the mean activation energy of the first reaction, associated with resin decomposition, results very close to that obtained for carbon-PEKK in inert conditions, despite a relatively higher standard deviation. The latter grows for the following two reactions, due to the quasi-linear decrease of the activation energy within their extent of conversion intervals.

The significant discrepancy obtained between the E_α evaluated with Starink and Friedman reveals the necessity to check these results with, at least, a third isoconversional method. In this sense, further analysis should be carried out for the activation energy estimation of the tested materials, under oxidative con-

$\bar{E}_a$	**Carbon-PEKK**		
$[kJ/mol]$	reac. 1	reac. 2	reac. 3
Starink	195.89 ± 8.23	181.83 ± 9.41	125.87 ± 23.42
Friedman	180.99 ± 43.04	158.01 ± 15.29	63.85 ± 41.55

Table 6: Mean activation energy $\bar{E}_\alpha$ corresponding to the three reaction observed for carbon-PEKK in oxidative atmosphere.

ditions, by considering more sophisticated methods, such as that proposed by Vyazovkin [44], based on the numerical integration of the temperature integral, of Eq. 6, on TG experimental data. From a qualitatively point of view, by comparing inert and oxidative case for carbon-phenolic, in the early degradation phase ($\alpha < 0.2$), associated with resin dehydration, one can see an activation energy range decrease of approximately 30% in oxidative results (see Figure 12). Such difference, in first approximation, might be related to combustion of the released products. On the contrary, the activation energy range of carbon-PEKK in the early degradation phase (first reaction) does not significantly vary from inert to oxidative conditions, despite a certain oscillation ($\sim$20% around Starink values) of Friedman values in Figure 13, highlighting a higher temperature stability, associated with ether and ketone bonds. It seems reasonable to suppose that carbon-PEKK is not affected by a significant pyrolysis before about 500 °C. Due to this characteristic, PEKK-based composites result to be very suitable solutions for fire protection, such fire barriers for interior aerospace components. On the other hand, the early degradation, with pyrolysis and char production, of phenolic resin, confirms its suitability for external thermal shields or internal rocket nozzles insulation.

In order to provide a complete kinetic description, besides the activation energy, also the preexponential factor A and the reaction model should be evaluated. The Friedman and compensation effect methods, considered in this work and typically used with isoconversional activation energy, are valid for the study of a sequence of isolated single-step reactions [19, 44]. Therefore, only carbon-PEKK in inert conditions results suitable for their application, whereas carbon-

phenolic shows a multi-step kinetic in both inert and oxidative atmospheres. However, for purpose of comparison, the kinetic triplet for the different reactions identified from DTG data are evaluated for the tested materials under inert conditions. The achieved results are presented in Table 7 and 8, respectively calculated with Friedman and compensation effect methods. As discussed in Section 3.3, the former assumes the general nth-order reaction model expression, thus estimating A and the reaction index n as the intercept and the slope of a least squares fitting of a rearranged form of Eq. 2, evaluated with the experimental data [45].

	Carbon-phenolic				**Carbon-PEKK**			
	$\bar{E}_a$ $[kJ/mol]$	A $[min^{-1}]$	n	R^2	$\bar{E}_a$ $[kJ/mol]$	A $[min^{-1}]$	n	R^2
Starink								
Reaction 1	154.58 ± 20.79	1.12×10^{12}	48.26	0.996	207.71 ± 6.57	4.23×10^{10}	1.50	0.958
Reaction 2	189.11 ± 24.09	2.93×10^{12}	6.29	0.998	n.d.	n.d.	n.d.	n.d.
Friedman								
Reaction 1	165.10 ± 25.57	1.50×10^{14}	51.32	0.996	213.88 ± 20.04	1.12×10^{11}	1.61	0.970
Reaction 2	201.66 ± 30.89	2.49×10^{13}	6.44	0.945	n.d.	n.d.	n.d.	n.d.

Table 7: Kinetic triplet evaluated with *Friedman* approach, based on the assumption of generic n-order reaction model $f(\alpha) = (1-\alpha)^n$ [45]. Carbon-phenolic and carbon-PEKK in inert atmosphere.

In Table 7, the fitting quality parameter R^2 is reported for each considered reaction. Moreover, the kinetic parameters are evaluated with both the isoconversional activation energies estimated with Starink and Friedman, reporting their mean value in the defined reaction interval. Despite the good fitting parameter obtained for phenolic reactions, the reaction index does not have physical meaning, due to the strong variation the the activation energy in the corresponding reaction α intervals. On the contrary, the results achieved for carbon-PEKK, which decomposition can be described, in first approximation, by a single-step global reaction, appear to be more realistic, keeping into account the uncertainty in experimental measurements. In particular, a better fitting parameter is achieved with Starink method, yielding a frequency factor and reaction index respectively equal to 4.23×10^{10} and 1.50.

The compensation effect method, whose results are reported in Table 8,

	Carbon-phenolic			Carbon-PEKK		
	$\bar{E}_a$ $[kJ/mol]$	A $[min^{-1}]$	$f(\alpha)$	$\bar{E}_a$ $[kJ/mol]$	A $[min^{-1}]$	$f(\alpha)$
Starink						
Reaction 1	154.58 ± 20.79	$3.86 \pm 4.72 \times 10^{8}$	n.d.	207.71 ± 6.57	$8.37 \pm 0.24 \times 10^{11}$	$3(1-\alpha)^{2/3}$
Reaction 2	189.11 ± 24.09	$3.90 \pm 0.25 \times 10^{12}$	n.d.	n.d.	n.d.	n.d.
Friedman						
Reaction 1	165.10 ± 25.57	$2.08 \pm 2.6 \times 10^{9}$	n.d.	213.88 ± 20.04	$2.00 \pm 0.04 \times 10^{12}$	$3(1-\alpha)^{2/3}$
Reaction 2	201.66 ± 30.89	$3.25 \pm 0.1 \times 10^{13}$	n.d.	n.d.	n.d.	n.d.

Table 8: Kinetic triplet evaluated with *compensation effect* method [19, 44]. Carbon-phenolic and carbon-PEKK in inert atmosphere.

exploits a graphical data comparison to identify the corresponding ideal reaction model. In Figure 14, one can see carbon-PEKK data plotted against few typical models, diffusion and geometrical types (see Table 3), considered for solid-state degradation. The single-step decomposition reaction of PEKK seems to obey, between α =0.1-0.8, to the contracting sphere model R3, see Table 8, for which the nucleation is assumed rapidly occurring on the surface of the crystal [42].

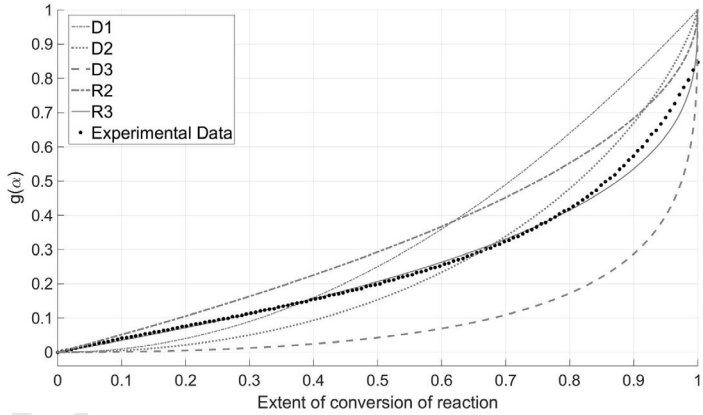

Figure 14: compensation effect method for decomposition model evaluation: carbon-PEKK in inert atmosphere, with regard to Starink activation energy estimated values.

Nevertheless, such result must be considered with caution, since a good matching with a specific model does not necessarily represent the real behavior [19, 44] and no confirmation was found in the literature, thus requiring further tests, with a wider range of temperature programs, for the assuring of the

achieved result. In fact, it is generally very hard to achieve perfect matching with theoretical models when dealing with polymeric materials [44]. In addition, one must remember that the non-isothermal heating rate applied by the thermogravimetric device significantly differs from the real situation in which the material is subjected to a direct flame. Therefore, the R3 model does not represent the exact description of the PEKK decomposition, but it is figured out as a starting hint for further analysis, more concentrated on the detailed kinetic, maybe exploiting also DSC analysis and flash pyrolysis with GC/MS, as well as to be used as preliminary approach for pyrolysis numerical simulations. In Table 8, the kinetic triplets are reported for the considered reactions. Due to the multi-step mechanism of carbon-phenolic, the calculated preexponential factors have not physical meaning and no any model correspondence was identified. With regard to carbon-PEKK, despite slight difference in the preexponential factors related to Friedman and Starink activation energy, the same model matching was obtained for both isoconversional methods. The value of frequency factor, presented in Table 8, corresponds to the average between the data of the three considered non-isothermal heating rates. No kinetic triplets evaluation was carried out for oxidative data, due to their complex kinetics, unsuitable for single-step-based approaches, such that of Friedman and compensation effect. In order to cover these lacks and improve the quality of the kinetic analysis, the next efforts will be focused on the implementation of model-fitting methods, that demonstrated a good ability to follow a multi-step reactions mechanism [19]. Therefore, a model-fitting treatment shall be applied to carbon-phenolic in inert conditions, as well as to carbon-PEKK to verify the achieved results. In addition, an isoconversional method based on the numerical integration of the temperature integral [44] will be implemented and applied to the oxidative experimental data, in order better evaluate isoconversional methods for activation energy estimation in presence of complex reactions patterns, such as that of polymer-based composite materials.

5. Conclusions

In this work, the kinetic degradation of two carbon-reinforced polymer resins was analyzed under inert and oxidative atmospheres. Thermogravimetric experimental results demonstrated two different behaviors for carbon-phenolic and carbon-PEKK composites. The first characterized by pyrolysis processes from a relative low temperatures (200-250 °C), while the second revealed a higher resistance to temperature, both in inert and oxidative environments, starting its decomposition at about 500 °C, after matrix melting phase. The higher performance of PEKK resin, attributed to the chemical structure of the monomer, make it as a promising material for aircraft components, especially where severe fire safety requirements must be accomplished. The activation energy estimation, carried out with two different isoconversional methods, provided a good reaction pattern representation accordingly with the experimental observations (reaction peaks identified by DTG curves), as well as values of the same order of that reported in the literature for the inert case. In such conditions, the PEKK decomposition seems to be driven by one single global reaction, whereas under oxidative atmosphere three clear peaks are observable from DTG experimental data, leading to suppose a degradation process described by three consecutive global reactions. Nevertheless, under oxidative conditions, the significant variation of the estimated isoconversional activation energy within the corresponding extent of conversion intervals, suggests the development of a more complex reaction pattern, characterized by multi-step reactions. Moreover, in oxidative case and for both the tested materials, a large difference is achieved between the E_α estimated by Starink and Friedman, revealing the necessity to check the results with a third isoconversional method, such as that of Vyazovkin, which exploits the numerical integration of the temperature integral. Concerning the estimation of reactions kinetic triplets, the implemented methods achieved valid results only for carbon-PEKK under inert atmosphere, providing hints for a possible model expression to describes the single-step dominant reaction identified. With regard to carbon-phenolic inert test and oxidative tests for both the materials,

the complex multi-step mechanisms observed cannot be properly analyzed with single-step-based methods, requiring the use of more sophisticated techniques. In the light of this, the next stage of this study, besides the above mentioned numerical integral isoconversional method for activation energy estimation, will be focused on the implementation of model-fitting approaches for a more appropriate analysis of multi-step reaction kinetics, as well as validation of the actual results. In addition, the characterization of PEKK resin will be improved by means of ongoing thermophysical properties analysis.

Acknowledgement

The authors desire to thank Philippe Gillard for availability and support in the thermogravimetric experiments and Jean-Claude Harge for SEM visualizations, all performed at the University Institute of Technology (IUT) of Bourges (France).

References

[1] U. Sorathia, R. Lyon, R. G. Gann, L. Gritzo, Materials and fire threat, SAMPE Journal 32 (3) (1996) 8–15.

[2] G. Marsh, Airbus takes on Boeing with reinforced plastic, Reinforced Plastics 51 (11) (2007) 26–27,29. doi:10.1016/S0034-3617(07)70383-1.

[3] G. Marsh, Bombardier throws down the gauntlet with CSeries airliner, Reinforced Plastics 55 (6) (2013) 22–26. doi:10.1016/S0034-3617(11)70181-3.

[4] E. A. S. A. (EASA), Annual Safety Review 2014, European Aviation Safety Agency, 2014.

[5] M. Tsoi, J. Zhuge, R.-H. Chen, J. Gou, Modeling and experimental studies of thermal degradation of glass fiber reinforced polymer composites, Fire and Materials 38 (2014) 247–263. doi:10.1002/fam.2178.

[6] J. Zhuge, J. Gou, R.-H. Cheng, J. Kapat, Finite difference analysis of thermal reponse and post-fire flexural degradation of glass fiber reinforced composites coated with carbon nanofiber based nanopapers, Composites Part A: Applied Science and Manufacturing 43 (2012) 2278–2288.

[7] M. Blazsó, Z. Czégény, C. Csoma, Pyrolysis and debromination of flame retarded polymers of electronic scrap studied by analytical pyrolysis, Journal of Analytical and Applied Pyrolysis 64 (2002) 249–261. doi:10.1016/S0165-2370(02)00035-9.

[8] N. Kim, D. Bhattacharyya, Development of fire resistant wool polymer composites: Mechanical performance and fire simulation with design perspectives, Materials & Design 106 (2016) 391–403. doi:10.1016/j.matdes.2016.06.005.

[9] ISO 2685:1998, Aircraft-Environmental Test Procedure for Airborne Equipment-Resistance to Fire in Designated Fire Zones, Tech. rep., International Organization for Standardization (1998).

[10] AC20-135, Power-plant installation and propulsion system component fire protection test methods, standards and criteria., Tech. rep., U.S. Department of Transportation - Federal Aviation Administration (1990).

[11] R. E. Lyon, Fire-resistant materials: research overview, resreport DOT/FAA/AR-97/99, Federal Aviation Administration: Airport and Aircraft Safety, Research and Development (1997).

[12] A. Johnston, R. Cole, A. Jodoin, J. MacLaurin, G. Hadjisohocleous, Evaluation of fire performance of composite materials for aircraft structural applications, in: International Committee on Composite Materials (ICCM), 1999.

[13] J. Zhuge, J. Gou, R.-H. Cheng, J. Kapat, Finite element modeling of post-fire flexural modulus of fiber reinforced polymer composites under constant

heat flux, Composites Part A: Applied Science and Manufacturing 43 (2012) 665–674.

[14] N. Grange, K. Chetehouna, N. Gascoin, S. Senave, Numerical investigation of the heat transfer in an aeronautical composite material under fire stress, Fire Safety Journal 80 (2016) 56–63. doi:10.1016/j.firesaf.2016.01.005.

[15] L. Torre, J. M. Kenny, a. M. Maffezzoli, Degradation behaviour of a composite material for thermal protection systems Part IExperimental characterization, Journal of Materials Science 33 (12) (1998) 3137–3143. doi:10.1023/A:1004399923891.

[16] N. Gascoin, P. Gillard, a. Mangeot, a. Navarro-Rodriguez, Detailed kinetic computations and experiments for the choice of a fuel-oxidiser couple for hybrid propulsion, Journal of Analytical and Applied Pyrolysis 94 (2012) 33–40. doi:10.1016/j.jaap.2011.12.002.

[17] N. Gascoin, G. Fau, P. Gillard, A. Mangeot, Experimental flash pyrolysis of high density polyethylene under hybrid propulsion conditions, Journal of Analytical and Applied Pyrolysis 101 (May 2013) (2013) 45–52. doi:doi:10.2514/6.2013-3833.

[18] S. Vyazovkin, K. Chrissafis, M. L. Di Lorenzo, N. Koga, M. Pijolat, B. Roduit, N. Sbirrazzuoli, J. J. Suñol, ICTAC Kinetics Committee recommendations for collecting experimental thermal analysis data for kinetic computations, Thermochimica Acta 590 (2014) 1–23. doi:10.1016/j.tca.2014.05.036.

[19] S. Vyazovkin, A. K. Burnham, J. M. Criado, L. A. Pérez-Maqueda, C. Popescu, N. Sbirrazzuoli, ICTAC Kinetics Committee recommendations for performing kinetic computations on thermal analysis data, Thermochimica Acta 520 (1-2) (2011) 1–19. doi:10.1016/j.tca.2011.03.034.

[20] M. P. Luda, a. I. Balabanovich, M. Zanetti, D. Guaratto, Thermal decomposition of fire retardant brominated epoxy resins cured with different nitrogen containing hardeners, Polymer Degradation and Stability 92 (2007) 1088–1100. doi:10.1016/j.polymdegradstab.2007.02.004.

[21] W. Zhang, X. Li, R. Yang, Pyrolysis and fire behaviour of epoxy resin composites based on a phosphorus-containing polyhedral oligomeric silsesquioxane (DOPO-POSS), Polymer Degradation and Stability 96 (10) (2011) 1821–1832. doi:10.1016/j.polymdegradstab.2011.07.014.

[22] M. R. Tant, H. L. N. McManus, M. E. Rogers, High-Temperature Properties and Applications of Polymeric Materials - An Overview, ACS Sympos. Series 603 (1995) 1–20.

[23] J. C. J. Bart, Polymer/additive analysis by flash pyrolysis techniques, Journal of Analytical and Applied Pyrolysis 58-59 (2001) 3–28. doi:10.1016/S0165-2370(00)00160-1.

[24] A. F. de Baas, Research road mapping in materials, Tech. rep., European Commission, Directorate-General for Research, Industrial Technology (2010).
URL http://ec.europa.eu/research/research-eu

[25] W. T. Engelke, C. M. Pyron, C. D. Pear, Thermal and mechanical properties of a nondegraded and thermally degraded phenolic-carbon composite, Tech. Rep. 23, National Aeronautics and Space Administration (1967).

[26] R. W. Humble, G. N. Henry, W. J. Larson, Space Propulsion Analysis and Design, 1st Edition, The McGraw-Hill Companies, Inc., 1995.

[27] J. S. Tate, S. Gaikwad, N. Theodoropoulou, E. Trevino, J. H. Koo, Carbon/Phenolic Nanocomposites as Advanced Thermal Protection Material in Aerospace Applications, Journal of Composites 2013 (2013) 1–9. doi:10.1155/2013/403656.

[28] G. Pulci, J. Tirillò, F. Marra, F. Fossati, C. Bartuli, T. Valente, Carbon–phenolic ablative materials for re-entry space vehicles: Manufacturing and properties, Composites Part A: Applied Science and Manufacturing 41 (10) (2010) 1483–1490. doi:10.1016/j.compositesa.2010.06.010.

[29] L. Riviere, N. Causse, A. Lonjon, É. Dantras, C. Lacabanne, Specific heat capacity and thermal conductivity of PEEK / Ag nanoparticles composites determined by Modulated-Temperature Differential Scanning Calorimetry, Polymer Degradation and Stability 127 (2015) 98–104. doi:10.1016/j.polymdegradstab.2015.11.015.

[30] B. Y. Lattimer, J. Ouellette, J. Trelles, Thermal Response of Composite Materials to Elevated Temperatures, Fire Technology 47 (4) (2011) 823–850. doi:10.1007/s10694-009-0121-9.

[31] G. Marsh, Fire-safe composites for mass transit vehicles, Reinforced Plastic 46 (9) (2002) 26–30. doi:10.1016/S0034-3617(02)80157-6.

[32] U. Sorathia, C. M. Rollhauser, W. A. Hughes, Improved Fire Safety of Composites for Naval Applications, Fire and Materials 16 (3) (1992) 119–125. doi:10.1002/fam.810160303.

[33] A. P. Mouritz, A. G. Gibson, Fire Properties of polymer composite materials, Springer, 2007. doi:10.1017/CBO9781107415324.004.

[34] A. Knop, L. A. Pilato, Phenolic Resins: Chemistry, Applications and Performance, 1st Edition, Springer-Verlag Berlin Heidelberg, 1985. doi:10.1007/978-3-662-02429-4.

[35] M. R. Ho, D. S. Z. Cheng, P. H. Fisher, K. R. Eby, S. B. Hsiao, H. K. Gardner, Crystal Morphology and Phase Identifications in Poly(Aryl Ether Ketone)s and Their Copolymers .2. Poly(Oxy-1,4- Phenylenecarbonyl-1,3-Phenylenecarbonyl-1,4-Phenylene), Macromolecules 27 (20) (1994) 5787–5793. doi:10.1021/ma00098a037.

[36] D. Mathijsen, Leading the way in thermoplastic composites, Reinforced Plastics 00 (00) (2015) 8–10. doi:10.1016/j.repl.2015.08.067.

[37] G. Marsh, Could thermoplastics be the answer for utility-scale wind turbine blades?, Reinforced Plastics 54 (1) (2010) 31–35. doi:10.1016/S0034-3617(10)70029-1.

[38] E. S. Oztekin, S. B. Crowley, R. E. Lyon, S. I. Stoliarov, P. Patel, T. R. Hull, Sources of variability in fire test data: A case study on poly(aryl ether ether ketone) (peek), Combustion and Flame 159 (4) (2012) 1720–1731. doi:10.1016/j.combustflame.2011.11.009.

[39] I. Chang, J. Lees, Recent Development in Thermoplastic Composites: A Review of Matrix Systems and Processing Methods, Journal of Thermoplastic Composite Materials 1 (3) (1988) 277–296. doi:10.1177/089270578800100305.

[40] B. Huang, S. Cheng, Q. Xi, M. Cai, Synthesis and characterization of novel copolymers of poly(ether ketone ketone) and poly(ether ketone sulfone imide), Polymer Bulletin 69 (6) (2012) 661–673. doi:10.1007/s00289-012-0753-7.

[41] P. Patel, T. R. Hull, R. W. Mccabe, D. Flath, J. Grasmeder, M. Percy, Mechanism of thermal decomposition of poly(ether ether ketone) (PEEK) from a review of decomposition studies, Polymer Degradation and Stability 95 (5) (2010) 709–718. doi:10.1016/j.polymdegradstab.2010.01.024.

[42] A. Khawam, D. R. Flanagan, Solid-state kinetic models: Basics and mathematical fundamentals, Journal of Physical Chemistry B 110 (35) (2006) 17315–17328. doi:10.1021/jp062746a.

[43] M. E. Brown, Introduction to Thermal Analysis - Techniques and applications, Kluwer Academic Publishers, 2001.

[44] S. Vyazovkin, Isoconversional Kinetics of Thermally Stimulated Processes, 1st Edition, Springer International Publishing, 2015.

[45] H. L. Friedman, Kinetics of thermal degradation of char-forming plastics from thermogravimetry. Application to a phenolic plastic, Journal of Polymer Science Part C: Polymer Symposia 6 (1) (1964) 183–195. doi:10.1002/polc.5070060121.

[46] T. Ozawa, A new method of analyzing thermogravimetric data, Bulletin of the Chemical Society of Japan 38 (11) (1965) 1881–1886. doi:10.1246/bcsj.38.1881.

[47] M. J. Starink, The determination of activation energy from linear heating rate experiments: A comparison of the accuracy of isoconversion methods, Thermochimica Acta 404 (1-2) (2003) 163–176. doi:10.1016/S0040-6031(03)00144-8.

[48] S. Feih, A. Mouritz, Tensile properties of carbon fibres and carbon fibre-polymer composites in fire, Composites Part A: Applied Science and Manufacturing 43 (5) (2012) 765–772. doi:10.1016/j.compositesa.2011.06.016.

[49] G. C. Vasconcelos, R. L. Mazur, B. Ribeiro, E. C. Botelho, M. L. Costa, Evaluation od decomposition kinetic of poly(ether-ether-ketone) by thermogravimetric analysis, Materials Research 17 (1) (2014) 227–235. doi:10.1590/S1516-14392013005000202.